Biophysical Chemistry 11 (1980) 461–473


# MEMBRANE BIOPHYSICS OF CHEMORECEPTION AND TAXIS IN THE PLASMODIUM OF *PHYSARUM POLYCEPHALUM*

Tetsuo UEDA, Tatsumi HIROSE and Yonosuke KOBATAKE
*Faculty of Pharmaceutical Sciences, Hokkaido University, Sapporo, Japan*

The threshold phenomena observed in chemoreception and taxis of the plasmodium of *Physarum polycephalum* were analyzed on the basis of physical chemistry. Various physicochemical concepts and rules, e.g. the Schulze-Hardy rule, the lyotropic number and the hydrophobic interactions, were shown to be applicable reasonably well to the physiological functions in *Physarum*. It was stressed that the structural change of the surface membrane induced by reception of chemical stimuli plays a decisive role in recognition and sensitivity to the external stimuli as well as the appearance of tactic movement in the amoeboid motility of *Physarum*.

## 1. Introduction

Microorganisms such as bacteria or protozoa can react to external chemical stimuli and exhibit appropriate behavior, as was discovered by Pfeffer and Engelman at the end of last century. Recent study on chemotaxis of bacteria with the aid of biochemical and genetical methods has put forward extensively our knowledge on molecular processes of chemoreception. Some specific proteins which are responsible for chemoreception have been isolated and identified in bacteria [1]. Specific binding of stimulus chemicals to receptor proteins in the membrane is considered as the initial process of chemoreceptions. Similar notion has been applied in the analysis of hormonal action and synaptic junction in higher organisms. Is the specific interaction between chemicals and binding sites the sole cause of the chemoreception?

As a complementary approach to this, one can try to elucidate the mechanism of chemoreception and taxis on the basis of physical chemistry where the processes of reception, recognition, and transduction are interpreted in terms of more general molecular interactions such as hydrophobic and/or electrostatic interactions between stimulus chemicals and membranes. Physicochemical techniques may be extended for use in microorganisms in living state without disrupting the cells, if appropriate organisms are used as experimental objects. In this connection, the true slime mold *Physarum polycephalum* is a suitable system as will be shown below.

The present article stresses that the physicochemical concepts are reasonably applicable to the interpretation of chemoreception and taxis in *Physarum*, and elucidate the following questions: How does the cell or surface membrane perceive molecular forces such as electrostatic and hydrophobic interactions as well as specific binding? How is the sensed information transduced into the motile system to result in tactic amoeboid movement in *Physarum*?

## 2. Plasmodium of *Physarum polycephalum* as a suitable experimental preparation

### *2.1. Morphology*

Plasmodium of *Physarum polycephalum* has characteristic features which admit application of physicochemical concepts as well as techniques to the living organisms. Fig. 1 shows typical shapes and dimensions of the plasmodia which are obtained by two different culture methods.

Large plasmodium (over 10 × 10 cm) migrates on agar gel by extending pseudopods and develops plasmodial veins when the organism is starved in surface culture (fig. 1a). Motility in the plasmodium belongs to typical amoeboid type. Cytoplasmic division does not associate

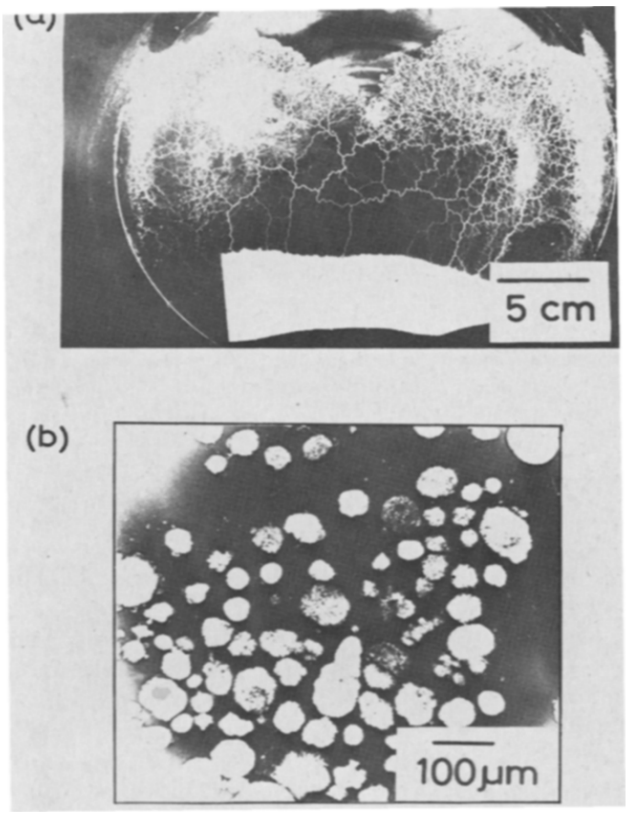


Fig. 1. Various shapes and dimensions of the plasmodia of *Physarum*. (a) Migrating plasmodium on agar gel in a petri dish. (b) Microplasmodia.

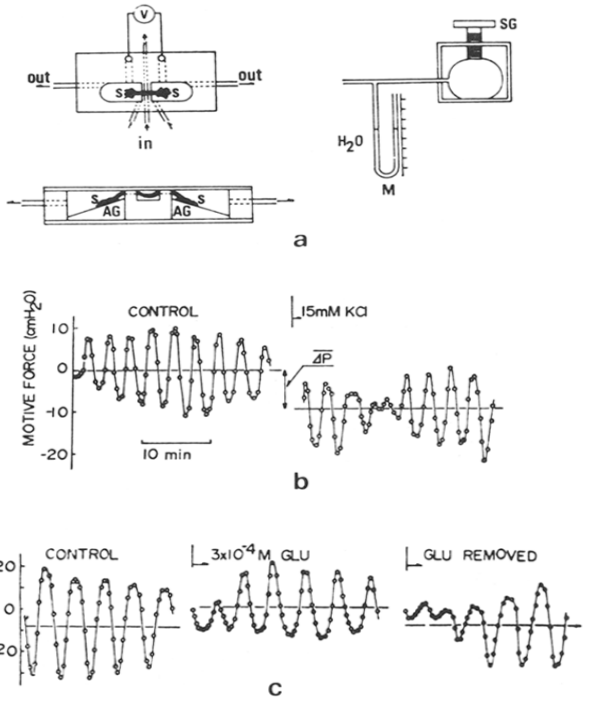


Fig. 2. Measurements of the motive force of the protoplasmic streaming and membrane potential by the double-chamber method. (a) Schematic illustration of the experimental arrangement. S: slime mold, AG: agar gel, M: manometer, V: potentiometer, SG: screw used for regulating pressure difference. (b), (c) Plasmodynamograms before and after the application of 15 mM KCl (a repellent) and 0.3 mM glucose (an attractant), respectively. $\overline{\Delta P}$ determines the tactic motive force in *Physarum*.

with nuclear division in the plasmodial stage, and separated plasmodia can easily fuse to form one plasmodium. These characteristics result in a large aggregate of protoplasm with no boundary cell wall separating each cells.

A characteristic back-and-forth streaming of the protoplasm takes place in the vein. The period of the oscillatory streaming is a few min and the maximum velocity of the protoplasmic streaming reaches more than 1 mm/s [2]. Biochemical study has shown that contractile proteins of actomyosin similar to muscular ones are responsible for this motility [3].

On the other hand, plasmodia cultured in liquid medium with vigorous shaking take spherical form having a diameter 50–100 $\mu$m, called microplasmodia (fig. 1b). Thus we may choose suitable form and dimension of the plasmodia at our disposal ranging between 50 $\mu$m and several cm. Or even, we can construct an arbitrary cell shape by making use of mutual fusibility of the plasmodia as seen in the double-chamber method as described below.

### *2.2. Measurements of chemotactic motive force and the membrane potential response*

Motive force of the protoplasmic streaming and changes in the membrane potential can be measured by using the double chamber method proposed by Kamiya about forty years ago [4], as depicted in fig. 2.

A plasmodium is separated into two portions hydrostatically as well as electrically through a narrow ditch except the strand portion at the middle which connects

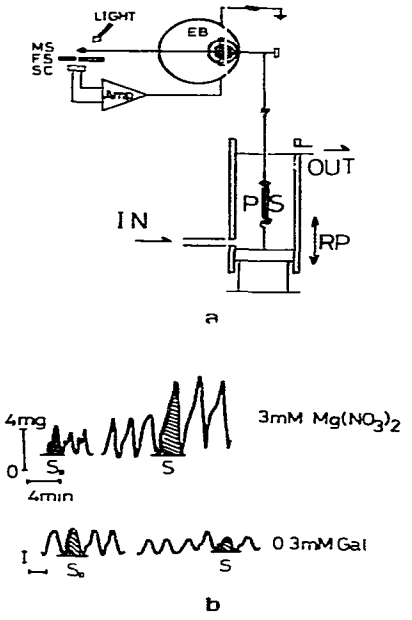


Fig. 3. Measurement of isometric tension in the plasmodial strand. (a) Schematic illustration of the experimental setup. PS: plasmodial strand, RP: rack-pinion, EB: electrobalance. (b) Time courses of the isometric tension before and after the application of 3 mM $Mg(NO_3)_2$ (a repellent) and 0.3 mM galactose (an attractant). *S* denotes the shaded area in the figure.

the two portions (fig. 2a). The basis of the measurement lies in the fact that the protoplasmic streaming in the middle strand can be stopped or counter-balanced by regulating a difference in hydrostatic pressures between two compartments, which therefore affords a quantitative measure of the motive force of the protoplasmic streaming. Application of a chemical to one compartment caused a deviation of the motive force of the protoplasmic streaming to either direction on the average, depending on attractants or repellents (fig. 2b, c). The averaged deviation of the motive force at the steady state, $\overline{\Delta P}$, is called the chemotactic motive force, and can be determined as a function of concentration of chemicals applied [5]. Note that the slime mold moved toward or away from the chemical if no pressure difference was applied and $\overline{\Delta P}$ was not zero.

One can measure the potential difference between two compartments. For this measurement, the plasmodium was placed on 1% agar gel containing 0.5 mM KCl to afford the electrical conductivity in the media.

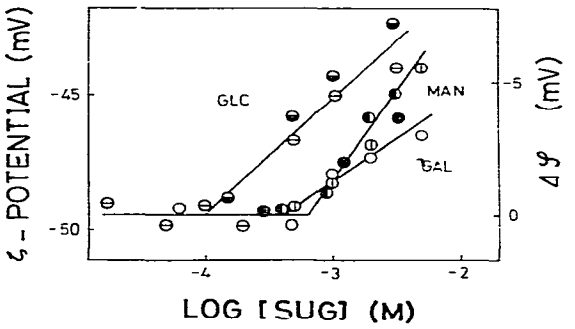


Fig. 4. Dependences of the zeta and membrane potentials on concentration of sugars. Zeta potential (ζ); ⊖: glucose, ⊕: mannose, ○: galactose. Membrane potential (Δψ); ⊖: glucose, ●: mannose, ●: galactose.

This concentration of KCl in the external medium did not interfere the chemoreception to other chemicals in the plasmodia. The potential difference between two chambers was picked up by a pair of calomel electrodes with salt bridges. Application of chemicals to one compartment caused a potential change when the concentration exceeded their respective threshold values, and removal of the chemical from the milieu recovered the original level of the potential. Potential difference determined by this method agreed with that measured by a microelectrode inserted into the cell so far as the change in the potential was concerned [6].

### *2.3. Tension generation in the plasmodial strand*

If we dissect a plasmodial strand a few cm long and put it into a tension meter, we can measure tension generation in the plasmodial strand (fig. 3a) [7,8]. This system may be regarded as a one-dimensional version of $\Delta P$ measurement and therefore as a simpler transduction system than the migrating organism. Fig. 3b illustrates the time courses of isometric tension before and after the application of chemicals. The effects can be quantified by taking the area, *S*, in tension curve as shown by the shaded area in the figure. The quantity *S* is proportional to chemical energy consumed during contraction in a period.

### *2.4. Electrophoretic mobility*

With use of microplasmodia, we can measure electro-

phoretic mobility, $u$, of a cell by applying the cell-electrophoresis under various external media [6]. With the help of the Helmholtz–Smoluchowski equation, we can calculate the zeta potential, $\zeta$;

$$\zeta = (4\pi\eta/D)u \,. \tag{1}$$

where $\eta$ and $D$ are the viscosity and the dielectric constant of the medium, respectively. Charge density, $\sigma$, at the surface of the membrane is calculated by use of the Gouy–Chapman equation:

$$\sigma = \left(\frac{DRT}{2000\pi}\right)^{1/2} \left(\sum_i [\exp(-z_i F\zeta/RT) - 1]\right)^{1/2}$$

$$\approx 2\left(\frac{DRT}{2000\pi}\right)^{1/2} \sqrt{C}\sinh\left(\frac{|z|F\zeta}{2RT}\right). \tag{2}$$

## 3. Changes in electrophoretic mobility of plasmodia in response to chemical stimuli

### *3.1. Response to sugars*

Fig. 4 shows the zeta and membrane potentials as a function of log concentration of sugars. Both the membrane potential, $\Delta\psi$, and zeta potential, $\zeta$, remain at a constant level until the concentration of the reagent reaches respective threshold, and then start to change in a positive direction as the concentration becomes higher than the threshold. The chemotactic movement of the slime mold took place at the same threshold concentration as the potential change, e.g. $1 \times 10^{-4}$ M for glucose, $3 \times 10^{-4}$ M for galactose, and $6 \times 10^{-4}$ M for mannose, respectively. These sugars act as attractants.

With the help of eq. (2), changes in zeta potential can be attributed to changes in the surface charge density, $\sigma$, because sugars used are non-electrolytes and hence the ionic strength in milieu stayed constant. Furthermore, the change in the surface charge density can probably be attributed to the conformational change of the receptor membrane. Thus, for example, in 1 mM glucose solution, 10–15% of the negative net charge is buried in the receptor membrane when a conformational change of the receptor membrane is induced by glucose reception. The gradual change in $\zeta$ may be interpreted as a successive increase of the number of domains, the conformation of which is changed by sugar reception, with increase of sugar concentration. A similar picture

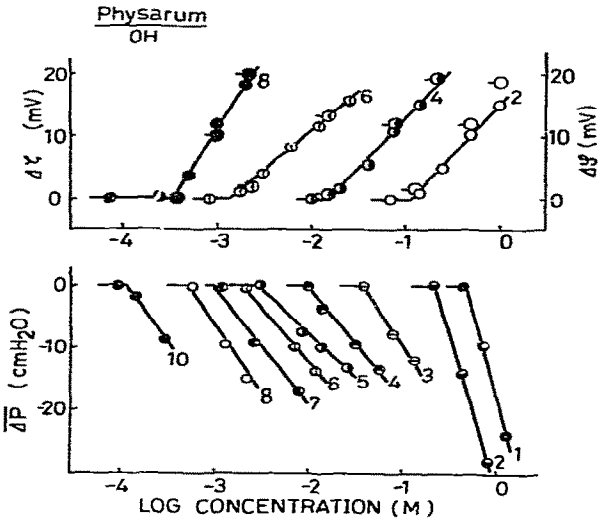


Fig. 5. Responses to $n$-alcohols in the plasmodium. Numbers in the figure indicate the number of carbon atoms in the homologous compounds.

is applied to receptions of hydrophobic substances, salts, nucleotides, etc.

Agreement between the changes of zeta and membrane potentials due to chemoreception with no appreciable change in membrane resistance for all chemical stimuli applied suggests that the change in intracellular potential stems mainly from the change in the interfacial potential at the membrane–solution interface rather than the ionic diffusion across the membrane. This notion is also confirmed in various chemoreceptive membranes [9].

### *3.2. Response to n-alcohols*

The upper trace of fig. 5 shows the concentration dependence of changes in membrane and zeta potentials of the plasmodia in response to $n$-alcohols with varying alkyl chain length [10]. The zeta and membrane potentials started to change at respective thresholds and depolarized almost linearly with $\log C$ above $C_{th}$. Tenfold increase of the concentration depolarized the membrane by about 20 mV.

$\overline{\Delta P}$ did not change until the concentration of chemicals reached the respective $C_{th}$, and increased (with negative sign) approximately linearly with $\log C$ above $C_{th}$. The threshold in chemotaxis agreed with that of potential

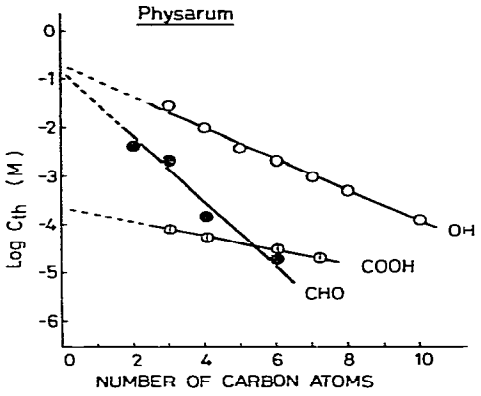


Fig. 6. Dependence of the recognition threshold on the number of carbon atoms. ○: *n*-alcohols, ●: *n*-aldehydes, ⊕: *n*-fatty acids.

response. These observations imply that the structural change of the membrane may trigger the chemotactic response as well as changes in charge density at the surface of the membrane.

### *3.3. Membrane and motility*

As shown in the lower trace of fig. 5, *n*-alcohols are repellents for the plasmodium of *Physarum*. Comparison of the results shown in figs. 4 and 5 (see also fig. 9) indicates that both attractants and repellents depolarized the membrane in a similar manner. This fact implies that the membrane potential does not govern the direction of movement in this organism, which contrast to the case of *Paramecium*, where depolarization and hyperpolarization of the membrane correspond to forward and backward cilial motions, respectively [11].

$\Delta P$ remained at a constant level of $\pm 10$ cm $H_2O$ for sugars, salts and nucleotides in a concentration higher than its own $C_{th}$. Contrary to these, hydrophobic substances such as *n*-alcohols, *n*-fatty acids and bitter substances caused gradual change in $\Delta P$ above $C_{th}$ well over 10 cm $H_2O$.

## 4. Hydrophobicity and heterogeneity of functional membranes

### *4.1. Dependence of the threshold concentration on alkyl-chain length*

As seen in fig. 5, the threshold concentration for *n*-alcohols decreased systematically with increase of the length of alkyl-chain. Similar observations can be made for *n*-aldehydes and *n*-fatty acids. Fig. 6 shows the dependence of the threshold on alkyl-chain length where $\log C_{th}$ is plotted against the number of carbon atoms, $n$, in the homologous compounds. Data follow each straight line for different functional groups at the end of the alkyl chain. Thus, we have the following empirical relation:

$$\log C_{th} = -An + B \,, \qquad (3)$$

where $A$ and $B$ are constants depending on the functional groups involved.

Table 1
Values of $\Delta\mu^0_{CH_2}$ in kcal/mol determined from eqs. (3) and (4) in various organisms

| Species | OH | CHO | COOH |
|---|---|---|---|
| Human olfaction | 0.95 | – | 0.1 |
| Rat | 0.9 | – | – |
| Blowfly | 0.71 | 0.72 | – |
| *Nitella* | 0.87 | 0.84 | 0.45 |
| *Tetrahymena* | 0.73 | 0.73 | 0.39 |
| *Paramecium* | 0.71 | – | – |
| *Physarum* | 0.45 | 0.9 | 0.2 |

### *4.2. Hydrophobicity of the membranes*

We can determine hydrophobicity and sensitivity of the chemoreceptive membrane from the empirical relation of eq. (3). Assuming that the stimulus chemicals are in partition equilibrium between membrane and solution phases, we can derive the parameter $A$ in eq. (3) as a function of difference in the standard chemical potentials of a $-CH_2-$group, $\mu^0_{CH_2}$, in the membrane and solution phases as follows:

$$A = (\mu^{0s}_{CH_2} - \mu^{0m}_{CH_2})/2.3RT = \Delta\mu^0_{CH_2}/2.3RT \,. \qquad (4)$$

Here, superscripts m and s indicate the quantities in the membrane and solution phases, respectively. Other symbols have their usual thermodynamic meanings. Eq. (4) reads that parameter $A$ in eq. (3) is a measure of the hydrophobicity of the membrane in problem [12].

Relationship expressed by eq. (3) is found to be applied to chemoreceptive membranes in a variety of organisms from bacteria to higher vertebrates. Thus, we can compare the hydrophobicity of various membranes

with use of eqs. (3) and (4) as summarized in table 1. We see some common features in this table. It may be noticed that the hydrophobicity of a biological membrane depends on the species of the end group of the compounds applied, and that the hydrophobicity of the membrane for COOH are about a half or less of those for OH and CHO for all organisms studied. These facts imply that the surface membrane of *Physarum* discriminates the end group of the chemicals at different receptor domain and that each domain has different hydrophobic characters. The membrane surface seems quite heterogeneous in character.

The hydrophobic interaction plays a role on the reception of chemicals other than homologous compounds such as *n*-alcohols or *n*-aldehydes. When the threshold in human olfaction, $T$, for various odorants are compared with those in chemoreceptions and taxis of lower organisms, $C_{th}$, we obtain the following relationship

$$\log T = \alpha \log C_{th} + \beta \,. \qquad (5)$$

Here, parameters $\alpha$ and $\beta$ are constants depending on biological species. Parameter $\alpha$ is given by the ratio of the hydrophobicities of biomembranes listed in table 1. The similar notion is applied to the response of various organisms against bitter substances [13].

The fact that the thresholds of olfactory reception and of bitter taste in higher animals are in good parallelism with chemoreception and taxis of protozoa indicates that these receptions are not governed by specific receptor molecules, but more general characters such as hydrophobicity of the chemoreceptive membranes are responsible for the reception of odor and bitter substances. This notion can also be applied to the actions of anesthetics [14].

## 5. Interactions involving water structure around the membrane surface

### *5.1. Discrimination of univalent cations and the lyotropic number of anions*

Plasmodium of *Physarum polycephalum* discriminates both cation and anion species of 1 : 1 salts. Fig. 7 shows the dependence of log $C_{th}$ on the lyotropic number of anions, $N$. The lyotropic numbers of anions were taken from the literature [15]. Fig. 7 shows that for various

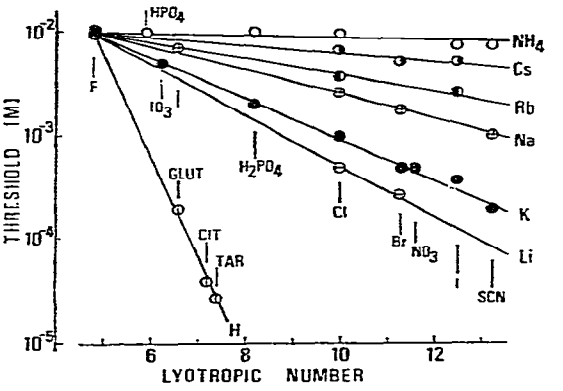


Fig. 7. Dependence of the recognition threshold, $C_{th}$, on the lyotropic number of anions, $N$.

salts containing a common cation and differing anions the plots of log $C_{th}$ versus the lyotropic number, $N$, of anions is linear; that is

$$\log C_{th} = -aN + b \,, \qquad (6)$$

in which $a$ and $b$ are constants depending on cation species and environment. We have determined that parameter $a$ decreases for the following sequence of cations:

$$\mathrm{H} > \mathrm{Li} > \mathrm{K} > \mathrm{Na} > \mathrm{Rb} > \mathrm{Cs} > \mathrm{NH_4} \,.$$

### *5.2. Interference between salt and sugar receptions*

Chemicals having different structures such as sugars and salts do not usually interfere each other in chemoreception. The presence of sugars in milieu, however, interferes the recognition thresholds for various salts in the plasmodium when the sugar concentration is higher than its own threshold concentration [16]. Double logarithmic plots of $C_{th}$ for univalent cation salts and sugar concentration, [SUG], gave different straight lines for different sugars:

$$\log C_{th} = a^* \log [\mathrm{SUG}] + \mathrm{const.} \qquad (7)$$

$$\text{when } [\mathrm{SUG}] \geqslant [\mathrm{SUG}]_{th} \,.$$

The parameter $a^*$ depends on species of monovalent cations and gives either positive or negative values. Here, $[\mathrm{SUG}]_{th}$ stands for the threshold concentration of the sugar added in the medium.

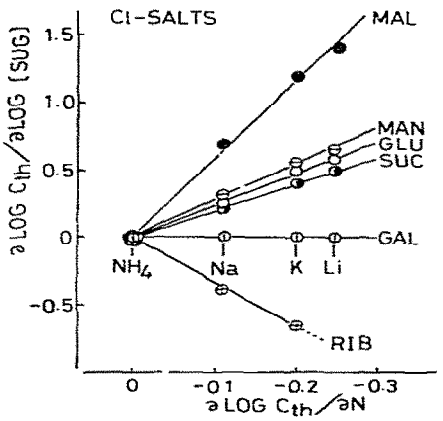


Fig. 8. Relationships between effects of coexisting sugars and the lyotropic number of anions on the thresholds for 1 : 1 type salts. ●: maltose, ⊖: mannose, ○: glucose, ◑: sucrose, ⊕: galactose, ⊖: ribose.

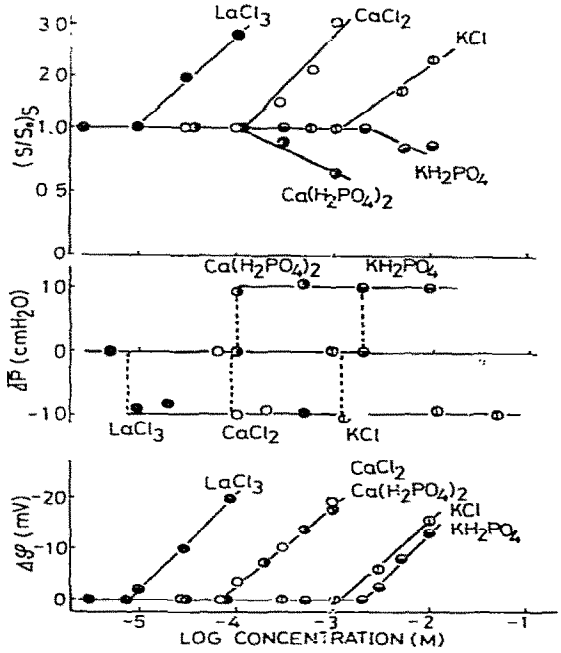


Fig. 9. Responses of the plasmodium of *Physarum* to various polyvalent salts. Tension generation ($S/S_0$), the motive force of taxis ($\overline{\Delta P}$), and the potential response ($\Delta\psi$).

### *5.3. Interpretation of the interference between salt and sugar receptions in terms of water structure*

Comparison of the parameters $a$ and $a^*$ in eqs. (6) and (7) reveals a close correlation between them. Fig. 8 shows the relation between $a$ ($=\partial \log C_{th}/\partial N$) and $a^*$ ($=\partial \log C_{th}/\partial \log [SUG]$) for various kinds of sugars and univalent cations.

The lyotropic number is a parameter which is closely correlated to the water structure in the sense that the iceberg structure increases with $N$. The correlation shown in fig. 8 indicates that the interference between salt and sugar receptions takes place through the water structure around the membrane. Recent physicochemical studies have indicated that sucrose and glucose tend to increase the structure of water, while ribose acts to disrupt the structure. These previous results are consistent with the results shown in fig. 8. Note that the interference appeared only when the coexisting chemicals exceeded their respective thresholds as expressed in eq. (7).

## 6. Electrostatic interactions in relation to chemoreceptive thresholds

### *6.1. The Schulze–Hardy rule in chemoreception*

Now it is the stage to discuss the electrostatic interactions between the plasmodial membrane and stimulus chemicals. Fig. 9 shows the concentration dependences of the tension generation in the plasmodial strand, $S/S_0$, of the chemotactic motive force, $\overline{\Delta P}$, and of the membrane potential, $\Delta\psi$, when the plasmodia were stimulated with various electrolytes [8]. The membrane potential did not change until the concentration of stimulus chemicals reached their respective thresholds, $C_{th}$. Above $C_{th}$, $\Delta\psi$ depolarized linearly with log $C$. Changes in $\Delta\psi$ agreed with those of zeta potential as described in section 3.2.

The threshold concentration decreased systematically with increase of valency of cation, $z$. We obtained a linear relationship with a slope $-6$ when $\log C_{th}$ is plotted against $\log z$, hence we have [5]

$$C_{th} = K_H z^{-6} . \qquad (8)$$

This relation is well known as the Schulze–Hardy rule in the field of colloid science, and $K_H$ is called as the Hamaker constant.

For the plasmodia of *Physarum polycephalum* of the wild type, the value of $K_H$ is 3 mM for all polyvalent

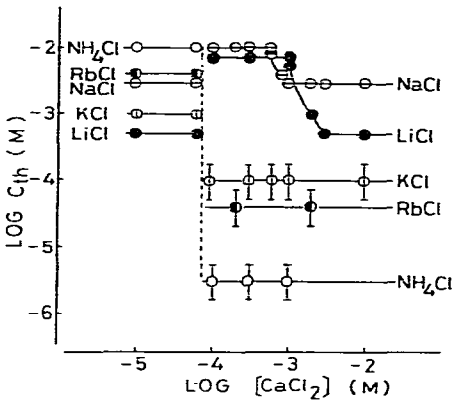


Fig. 10. Effects of the coexisting $CaCl_2$ concentration in media on the threshold of 1 : 1 type salts.

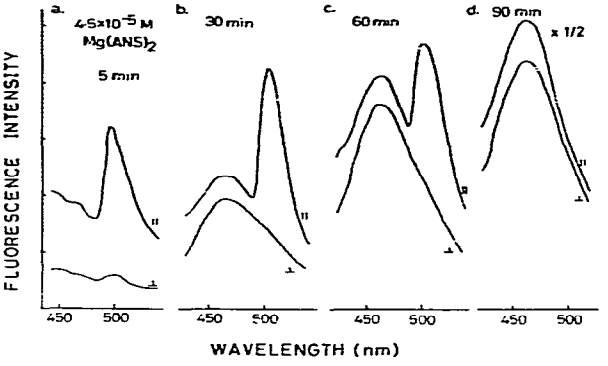


Fig. 11. Time course of the spectral pattern of ANS fluorescence. A white plasmodium was dipped in $4.5 \times 10^{-5}$ M Mg(ANS)$_2$. ∥ and ⊥ indicate parallel and vertical components of fluorescence intensities with respect to the polarized excitation light.

cations examined, while a white plasmodium described below (strain Lu 647 × Lu 861) has two distinct $K_H$ values of 3 mM for Ca, La and Th (group I) and of 0.2 mM for Na, K, Mg, Mn and Al (group II) [17].

According to the theoretical interpretation for the Schulze–Hardy rule, the instability of lyophobic colloids appears as a result of competition between repulsive force due to the electrical double layer and attractive force of the van der Waals interaction [18]. However, structural similarity between colloidal system and the slime mold might not be stressed at present.

### *6.2. Correlation between tension generation and tactic movement*

The relative tension of the plasmodial strands, $S/S_0$, decreased when an attractant [e.g. $Ca(H_2PO_4)_2$ or $NaH_2PO_4$] is applied to the plasmodium, whereas $S/S_0$ increased with reception of a repellent [$CaCl_2$, NaCl, or other inorganic salts]. With increase of the stimulus concentration, $S/S_0$ did not change until the threshold, $C_{th}$, and either increased or decreased gradually above $C_{th}$. Contrary to this, chemotactic motive force, $\overline{\Delta P}$, changed at $C_{th}$ almost in an all-or-nothing manner by +10 cm $H_2O$ for attractant and by −10 cm $H_2O$ for repellent. Similar changes in $\overline{\Delta P}$ and $S/S_0$ were observed for sugars and nucleotides.

Comparison between $S/S_0$ and $\overline{\Delta P}$ affords a possible explanation for the mechanism of chemotactic movement in the plasmodium, although the relation between the two is non-linear. Local application of an attractant reduces the tension at that portion, which produces a difference in internal hydrostatic pressures pushing the plasma sol to move towards that portion. Thus, a positive taxis occurs, and vice versa for negative taxis. Similar mechanism is applicable to the phototactic movement in *Physarum* [19].

### *6.3. Interference between salt receptions in Physarum*

A nature of the threshold phenomena in the reception of polyvalent cations can be made clear by the interference experiments between receptions of two different salts. Fig. 10 shows the effects of coexisting $Ca^{2+}$ in media on the thresholds of various 1 : 1 type salts. Ca gave rise to no effect on the chemoreception of 1 : 1 type salts until Ca concentration reached its own threshold, $6 \times 10^{-5}$ M. Above $C_{th}$ of Ca, the interference appeared discontinuously. $C_{th}$ for $NH_4Cl$, for example, became abruptly more than one thousand times lower [20].

When different polyvalent cations such as Mg, La and Th coexisted, similar discontinuous effects on $C_{th}$ for 1 : 1 type salts were observed at respective thresholds of polyvalent cations.

## 7. Fluorescence analysis of ANS in chemoreception

Fluorescence technique is applied to the study of

molecular processes of chemoreception of the surface membrane in white plasmodia, a mutant of *Physarum polycephalum* (strain Lu 647 × Lu 861).

We consider ANS salts as chemical stimuli with a fluorophore which fluoresces only in hydrophobic environments such as in the plasmodial membrane.

### *7.1. Fluorescence signals of extrinsic ANS accompanying with chemoreception*

The frontal region of the migrating plasmodium was cut with agar gel, put in a chamber and placed onto a fluorospectrophotometer. Thus, we measure fluorescence light emitted from a sheat of the plasmodium. Fig. 11 shows changes in spectral pattern of ANS fluorescence with time when $4.5 \times 10^{-5}$ M $Mg(ANS)_2$ was applied to the white plasmodium. Just after the application, ANS spectra exhibited a maximum at 500 nm. As time went on, fluorescence at 460 nm grew larger and larger and became the major emission at the final stage. Application of $Mg(ANS)_2$ below $C_{th}$ ($=1 \times 10^{-5}$ M) induced no time variation in the spectral pattern and fluoresced at 500 nm such as shown in fig. 11a [17]. Similar variation in spectral pattern with time was observed with NaANS applied to the white plasmodium. In this case, the threshold appeared at $1 \times 10^{-4}$ M, which agreed with $C_{th}$ determined from the membrane potential response (see fig. 12).

### *7.2. Nature of structural change in the plasmodial membrane by chemoreception*

According to the physicochemical studies of ANS fluorescence, the maximum emission of ANS locates at 500–520 nm in polar environments, and shifts to 460 nm in hydrophobic media. Based on these characteristics of ANS, the data shown in fig. 11 are interpreted as follows. Below $C_{th}$, the surface membrane of the plasmodia is predominantly hydrophilic and hence penetration or binding of ANS molecules at the membrane surface is prevented. On the other hand, hydrophobic portion on the membrane having access to ANS increases rather discontinuously above $C_{th}$. This picture is consistent with the results of adhesive properties of the plasmodia, i.e. adhesion of the plasmodia to hydrophobic substrate such as polypropylene surface increases above $C_{th}$ for each chemicals added in media [21].

Data shown in fig. 11 are also analysed in terms of

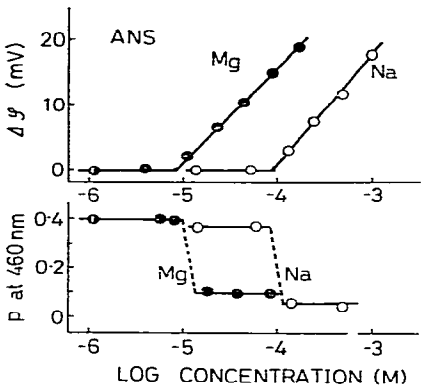


Fig. 12. Concentration dependences of the membrane potential, $\Delta\psi$, and the fluorescence polarization, $p$, when the plasmodium was exposed to Mg and Na salts of ANS.

the fluorescence polarization, $p$, which is a parameter of the membrane fluidity as regards to the binding sites of ANS on the membrane. The parameter $p$ is defined as follows:

$$p = (I_{\parallel} - I_{\perp})/(I_{\parallel} + I_{\perp}) , \qquad (9)$$

where $I_{\parallel}$ and $I_{\perp}$ stand for the parallel and perpendicular components of the fluorescence intensity with respect to the incident light.

In fig. 12, a comparison is made between changes in the membrane potential and in the fluorescence polarization, $p$, at 460 nm when $Mg(ANS)_2$ or NaANS was applied to the white plasmodium. The membrane potential changed in a similar manner as the corresponding chlorides and depolarized linearly with $\log C$ above the respective $C_{th}$. Contrary to the case of the membrane potential, $p$ changed in an all-or-nothing manner at the threshold. The value of $p$ decreased from 0.4 to 0–0.1 both for Mg and Na salts of ANS.

Fluorescence polarization, $p$, is related to the rotational motion of the chromophore by the well known Perrin's equation,

$$1/p - 1/3 = (1/p_0 - 1/3)(1 + 3\tau/\rho) , \qquad (10)$$

where $p_0$ is a constant, $\tau$ the fluorescent life time and $\rho$ the rotational relaxation time of the solute. $\rho$ is proportional to the microviscosity of the medium surrounding the chromophore. Assuming that $\tau$ stays constant, we may attribute the decrease in $p$ to a lowering of microviscosity of the membrane. Thus, the data

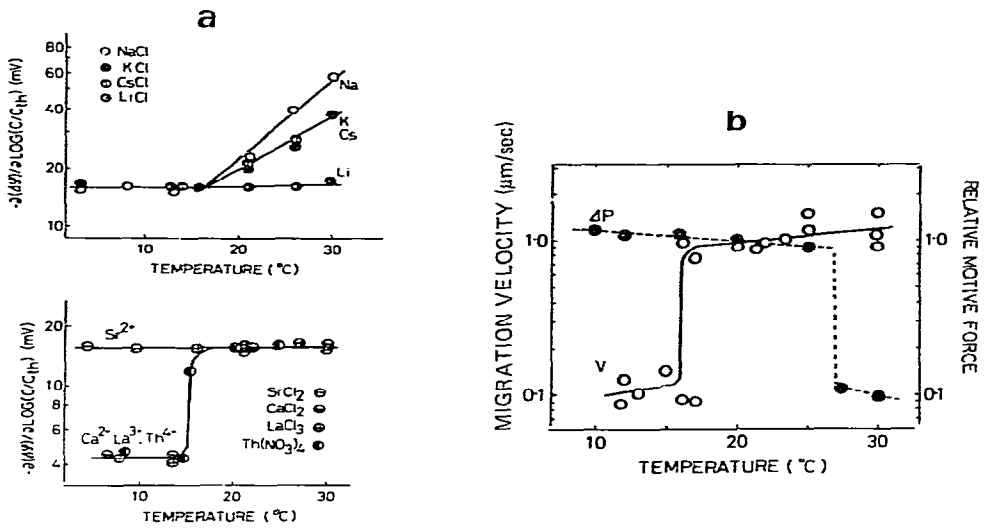


Fig. 13. Temperature dependences of potential response $R = \partial \Delta\psi / \partial \log (C/C_{th})$ (a), migration velocity (○) and the motive force (●) of protoplasmic streaming (b).

shown in fig. 12 indicate that the chemoreceptive membrane becomes more fluid discontinuously on reception of Mg and Na salts.

In white plasmodia, addition of Ca, La or Th salts caused an increase in $p$, while that of $NH_4$, K and Mg decreased $p$ for extrinsic ANS. This fact classifies cations into two groups: group I; Ca, La and Th, and group II; Na, K, $NH_4$, Mg and Al. This classification agrees with that based on the Schulze–Hardy rule as shown in section 6.1.

## 8. Thermal transition of the membrane and its effect on chemoreception and motility of *Physarum*

Critical phenomena have also been observed in membrane activities of the plasmodium by varying temperature [22]. Fig. 13a shows the temperature dependence of the magnitude of potential response defined by $R = \partial \Delta\psi / \partial \log C$ ($C > C_{th}$). On decreasing the temperature, $R$ changed abruptly from 18 mV/decade to 4.2 mV/decade for Ca, La and Th salts at $T_c = 15°C$, while that remained constant for Sr salt. For monovalent salts, $R$ remained at a constant level of 18 mV/decade below $T_c$ and increased above $T_c$. Note that the changes in the membrane potential agreed with those in the zeta potential even in this case.

Fig. 13b shows a comparison of the magnitude of the motive force of the protoplasmic streaming and the migration velocity at different temperatures. With decrease of temperature the amplitude of $\Delta P$ increased slightly, while the migration velocity decreased sharply by a factor of 1/10 at $T_c = 15°C$. The presence of the critical temperature in the locomotion may be attributed to the alteration of the membrane structure due to temperature variation.

## 9. Manipulation of intracellular components

Making use of the fact that the endoplasm in a plasmodial vein flows passively according to the gradient of the hydrostatic pressure in an ectoplasmic tube, we can replace endoplasm with an appropriate artificial solution without suppressing the contractility [23]. By this manipulation, we can study the effects of chemicals in the internal fluid on the contractility of plasmodial strands.

### *9.1. Replacement of endoplasm with artificial media*

Fig. 14 shows experimental arrangement for measuring the tension of the strand before and after the injection of artificial solution. The point is that the injection

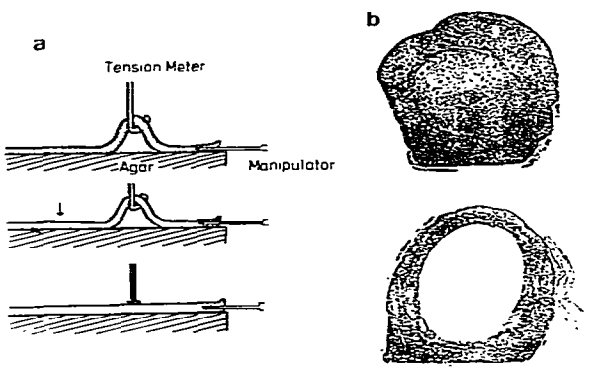


Fig. 14. Replacement of endoplasm with an artificial solution in the plasmodial vein. (a) Schematic illustration of the experimental setup and procedure. (b) Cross sections of the plasmodial vein before and after the injection.

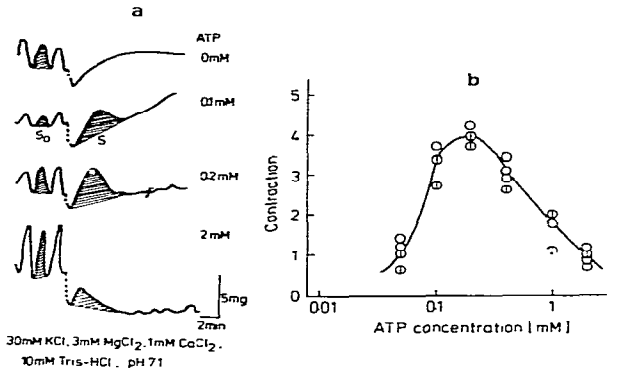


Fig. 15. Effects of injected ATP on tension generation of a plasmodial strand. (a) Time courses of tension generation before and after the injection. Concentration of ATP is denoted in the figure. The other components in the injected solution are: 30 mM KCl, 3 mM $MgCl_2$, 1 mM $CaCl_2$, 10 mM Tris-HCl, pH 7.1. (b) Dependence of the relative contraction ($S/S_0$) on the ATP concentration injected in the vein.

should be performed so rapidly as to be completed before the plasma sol turns to gel, and at the same time the applied pressure is not so strong to collapse the ectoplasmic tube. Owing to the viscoelastic properties of the ectoplasmic wall, we can replace plasma sol with an artificial solution more than 3 cm along the vein without blowing up the strand in the radial direction [23,24]. Fig. 14b shows a cross section of the plasmodial strand before and after the injection of an aqueous solution. We can see that predominant part of the endoplasm has been replaced with an artificial solution by this operation. The remaining ectoplasmic tube retains the contractile activity.

### *9.2. Effects of injected ATP, Ca and high salt solutions on tension generation*

Fig. 15a shows the time course of tension generation before and after the injection of ATP. Experimental conditions are described in the figure caption. An injection of the solution without ATP suppressed the oscillatory contraction of the strand. Addition of ATP induced a transient contraction. Its duration was about 5–6 min, 2–3 times longer than the period of normal oscillation of the tension of the strand. Injection of high concentration of ATP reduced the tension generation. This effect was attributed to the collapse of the ectoplasmic tube due to high ATP concentration.

Fig. 15b shows the dependence of the tension on the concentration of injected ATP, where contraction was expressed by $S/S_0$. $S$ and $S_0$ denote the shaded area in fig. 15a. From the figure, we can see that optimal contraction was realized at about 0.2 mM ATP. We may expect that a living cell consumes its chemical energy most effectively. Thus, we conclude that the intracellula. ATP level is maintained at the optimal contraction, i.e., at 0.2 mM ATP. In the subsequent study, ATP concentration is fixed at this level.

Fig. 16a shows the time course of tension generation when various levels of $Ca^{2+}$ were injected into the plasmodium. $Ca^{2+}$ level was maintained by CaEGTA buffer (10 mM). Increase of $Ca^{2+}$ level caused a contraction of the strand on the average, but the oscillation of the tension retained. Fig. 16b shows concentration dependence of injected $Ca^{2+}$ on the contractility of the plasmodial strand. Contraction took place above $2 \times 10^{-7}$ M $Ca^{2+}$. If we could inject an appropriate physiological solution compatible with the protoplasm into the plasmodia, tension generation would continue without any change in the contractibility. By this method, we could estimate that intracellular free $Ca^{2+}$ level is in the order of $10^{-6}$ M in the plasmodium of *Physarum*.

The effects of injected ATP and $Ca^{2+}$ on tension generation may be compared to those of ATPase activity of plasmodial actomyosin in vitro [25]. Activity of the ATPase is known to become optimum at 0.2 mM ATP in the presence of $Ca^{2+}$ and its threshold is about $1 \times 10^{-7}$ M $Ca^{2+}$. These results indicate that the injected

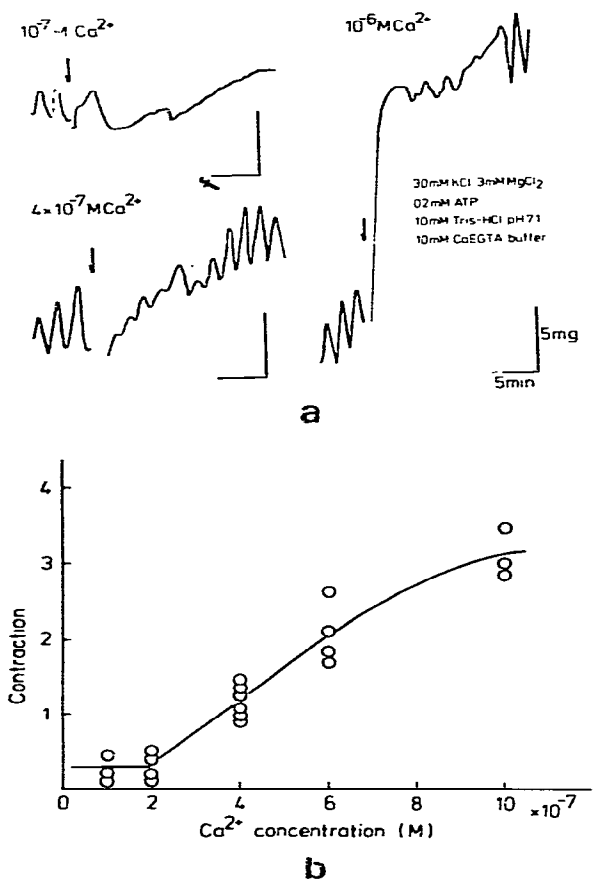


Fig. 16. Effects of injected $Ca^{2+}$ concentration on tension generation. (a) Time course of tension generation before and after the injection of $Ca^{2+}$. Free $Ca^{2+}$ level in the injected solution was regulated by 10 mM CaEGTA buffer and denoted in the figure. (b) Dependence of the contraction on $Ca^{2+}$ concentration. The contraction of the strand is reduced by the amplitude of each oscillating tension before injection in this figure.

chemicals act directly on the motile system in the strand. Note that the threshold for $Ca^{2+}$ and ATP in chemotaxis applied externally are 10 and 100 times higher than those of chemicals injected inside the cell.

Injection of high salt solution decreased the tension generation and diminished the oscillatory contraction [26]. Fig. 17b shows concentration dependence of the relative tension for chloride salts of various alkalimetal ions. The effects of injected salts on tension depended on cation species in the following sequence:

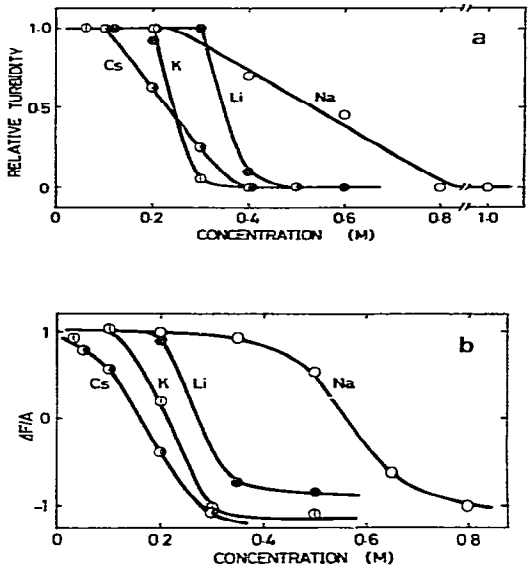


Fig. 17. Effects of high salt solutions in contractile systems in *Physarum*. (a) Relative turbidity of the plasmodial myosin B as a function of chloride salts of alkalimetal ions. (b) Changes in the reduced tension generation ($\Delta F/A$) induced by injection of salts as a function of concentration. Here, $A$ stands for the amplitude of oscillating tension before the injection.

$$Cs > K > Li > Na\ .$$

Fig. 17a shows concentration dependence of solubility of myosin B extracted from the plasmodium of *Physarum*. Solubility is expressed by the relative turbidity of the myosin B solution. Solubility of myosin B also showed cation specificity with the following sequence:

$$Cs > K > Li > Na\ .$$

Comparison of the data shown in fig. 17a and b, indicates that the effect of high concentration of salt solution injected in the strand on the decrease of tension generation is ascribed to the solubilization of filamentous actomyosin in the ectoplasmic tube of the plasmodium. In fact, cross section of the plasmodial strand exhibits very thin layer of ectoplasm when a salt solution of high concentration is perfused internally.

## 10. Conclusion

The chemoreception and taxis in the plasmodia of *Physarum polycephalum* were studied by applying

physicochemical concepts. Results are:

(1) The electrophoretic mobility of microplasmodia changed in response to sugars, nucleotides, hydrophobic substances and salts. Negative charge density at the membrane surface decreased in response to chemical stimuli. Changes in the membrane and zeta potentials agreed with each other for all cases examined.

(2) Recognition threshold decreased systematically with increase of the length of alkyl-chain in homologous compounds. From the empirical relation, the hydrophobicity of the chemoreceptive membranes was evaluated.

(3) Effects of differing anions in reception of 1 : 1 type salts were expressed by a simple formula by using the lyotropic number of anions.

(4) Interference between sugar and salt receptions was interpreted in terms of water structure at the membrane-solution interface.

(5) Effects of valency of polyvalent cations were expressed by the Schulze–Hardy rule. Discontinuous transition of the membrane at the thresholds was demonstrated by interference experiments and by fluorescence analysis of ANS.

(6) Thermal transition of the plasmodial membrane affected sharply on the chemoreception and motility of *Physarum*.

(7) Chemotaxis of the plasmodium is explained by the contractility of the strand. Injection studies showed that ATP, $Ca^{2+}$ and high salt concentration acted to modulate the contractility of the strand.

All these results indicate that the structural change of the surface membrane plays an indispensable role in recognition of chemicals and appearance of motility in the plasmodium of *Physarum polycephalum*.

## References


[1] J. Adler, Science 166 (1969) 1588.
[2] N. Kamiya, Protoplasmatologia 8 (1959) 1.
[3] S. Hatano, Advan. in Biophys. 5 (1973) 143.
[4] N. Kamiya, in: The structure of protoplasm (Iowa State University Press, Ames, Iowa, 1942).
[5] T. Ueda, K. Terayama, K. Kurihara and Y. Kobataka, J. Gen. Physiol. 65 (1975) 227.
[6] M. Hato, T. Ueda, K. Kurihara and Y. Kobatake, Biochim. Biophys. Acta 426 (1976) 73.
[7] N. Kamiya, R.D. Allen and R. Zeh, Acta Protoxoologiaa 11 (1972) 113.
[8] T. Ueda, M. Muratsugu, K. Kurihara and Y. Kobatake, Exp. Cell Res. 100 (1976) 337.
[9] N. Kamo, M. Miyake, K. Kurihara and Y. Kobatake, Biochim. Biophys. Acta 367 (1974) 1.
[10] T. Ueda and Y. Kobatake, Cytobiologie 16 (1977) 16.
[11] R. Eckert, in: Behaviour of microorganisms (Plenum Press, London-New York, 1973).
[12] T. Ueda and Y. Kobatake, J. Membrane Biol. 34 (1977) 351.
[13] M. Ataka, A. Tsuchii, T. Ueda, K. Kurihara and Y. Kobatake, Comp. Biochem. Physiol. 61A (1978) 109.
[14] P. Seeman, Pharmacol. Rev. 24 (1972) 583.
[15] A. Voet, Chem. Rev. 20 (1939) 169.
[16] K. Terayama, T. Ueda, K. Kurihara and Y. Kobatake, J. Membrane Biol. 34 (1977) 369.
[17] T. Ueda and Y. Kobatake, Biochim. Biophys. Acta, 557 (1979) 199.
[18] E.J. Verway and J.Th.G. Overbeek, in: Theory of stability of lyophobic colloids. (U.M. Elsevier, Amsterdam, 1948).
[19] M. Hato, T. Ueda, K. Kurihara and Y. Kobatake, Cell Structure and Function 1 (1976) 155.
[20] K. Terayama, K. Kurihara and Y. Kobatake, J. Membrane Biol. 37 (1977) 1.
[21] N. Ishida, K. Kurihara and Y. Kobatake, Cytobiologie 15 (1977) 269.
[22] T. Ueda and Y. Kobatake, Cell Structure and Function 3 (1978) 129.
[23] T. Ueda and K. Götz von Olenhusen, Exp. Cell. Res. 116 (1978) 55.
[24] T. Ueda, K. Götz von Olenhusen and K.E. Wohofarth-Bottermann, Cytobiologie 18 (1978) 76.
[25] T. Kato and Y. Tonomura, J. Biochem. 77 (1975) 1127.
[26] T. Hirose, T. Ueda and Y. Kobatake (1979) in preparation.